

Article

Expected Changes in Rainfall-Induced Landslide Activity in an Italian Archaeological Area

Evelina Volpe ¹, Stefano Luigi Gariano ¹, Luca Ciabatta ¹, Yaser Peiro ² and Elisabetta Cattoni ^{2,*}

¹ Research Institute for Geo-Hydrological Protection, National Research Council, 06128 Perugia, Italy; evelina.volpe@irpi.cnr.it (E.V.); stefano.luigi.gariano@irpi.cnr.it (S.L.G.); luca.ciabatta@irpi.cnr.it (L.C.)

² eCampus University, 22060 Novedrate, Italy; yaser.peiro@studenti.uniecampus.it

* Correspondence: elisabetta.cattoni@uniecampus.it

Abstract: Cultural heritage is one of the most exceptional resources characterizing the Italian territory. Archaeological heritage, i.e., the archaeological sites with different types of archaeological artifacts, strongly contributes to enriching the national and international cultural heritage. Nevertheless, it is constantly exposed to external factors, such as natural deterioration, anthropic impact, and climate-related hazards, which may compromise its conservation. In Italy, many archaeological areas are affected by significant soil settlements that involve a large part of monuments. This paper focuses on the landslide hazard assessment of the archaeological site of Pietrabbondante (Molise region, Italy). The impact of the expected rainfall regimes, according to the EURO-CORDEX projections, on slope stability conditions were evaluated through the application of a physically based model that couples a hydraulic and a mechanical model to evaluate slope stability evolution due to pore pressure changes. Given the unavoidable lack of knowledge of the geotechnical soil properties in an archaeological heritage area, the proposed method considered the random uncertainty of soil parameters by means of a probabilistic approach in order to assess the stability conditions in terms of probability of occurrence of a landslide. The results of this study provide a reference for the safety assessment and preventive conservation of archaeological areas characterized by high cultural value.

Keywords: cultural heritage; rainfall projections; probabilistic approach; reliability analysis; climate change



Citation: Volpe, E.; Gariano, S.L.; Ciabatta, L.; Peiro, Y.; Cattoni, E. Expected Changes in Rainfall-Induced Landslide Activity in an Italian Archaeological Area. *Geosciences* **2023**, *13*, 270. <https://doi.org/10.3390/geosciences13090270>

Academic Editors: Salvatore Grasso, Deodato Tapete and Jesus Martinez-Frias

Received: 29 June 2023

Revised: 10 August 2023

Accepted: 4 September 2023

Published: 7 September 2023



Copyright: © 2023 by the authors. Licensee MDPI, Basel, Switzerland. This article is an open access article distributed under the terms and conditions of the Creative Commons Attribution (CC BY) license (<https://creativecommons.org/licenses/by/4.0/>).

1. Introduction

Italy has one of the vastest cultural heritages in the world, including 4000 museums, 6000 archaeological sites, 24 national parks, 23 marine areas, and 58 World Heritage sites. Monuments, visited every year by millions of people, represent an important resource, supporting its social and economic development. According to data from the State General Accounting Office, the economic dimension of Italian cultural heritage is about EUR 986 billion between financial and non-financial assets.

At the same time, the vast Italian heritage is constantly exposed to natural and anthropic deterioration and also affected by climatic and environmental changes [1]. Climate change and the consequent increase of frequency and intensity of weather events [2,3] constitute a significant threat to the sustainability of many heritage resources all over the world [4,5]. Climate change may also influence the frequency and intensity of landslides with significant widespread impacts [6], particularly in Italy [7].

Different authors have already evaluated the impact of slope instabilities on cultural heritage worldwide, such as in the Derwent Valley Mills, the United Kingdom [8], Petra, Jordan [9], and the Greek Island of Crete [10], also considering a climate change perspective [11–14].

A protocol signed by the Italian Institute for Environmental Protection and Research (ISPRA, *Istituto Superiore per la Protezione e la Ricerca Ambientale*) and the High Institute

for Conservation and Restoration (ISCR, *Istituto Superiore per la Conservazione e il Restauro*) revealed that (only in 2013) on 100,258 observed cultural assets, 5500 have been exposed to landslide risk (about 6.6%) and 11,155 (about 11%) to flooding risk [15].

According to the data published by ISPRA [16], the amount of cultural heritage assets exposed to landslide and flood risk has been increasing during the recent years (Figure 1). Moreover, as shown in Figure 1, the percentage of the distribution of cultural heritage exposed to the highest level of risk has been increasing. In the case of landslide risk, the exposure of cultural heritage assets to the very high hazard level has increased from 12% in 2015 to 14% in 2021.

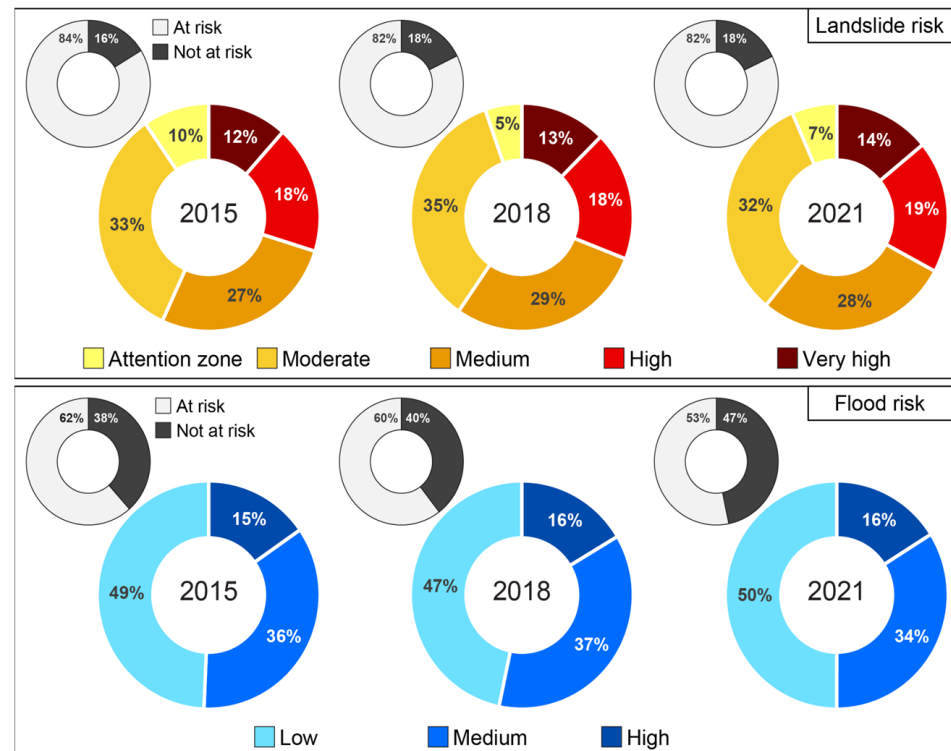


Figure 1. Distribution of cultural properties in different landslide and flood hazard classes in 2015, 2018, and 2021. Source: [16].

In 2021, 38,000 cultural assets have been subjected to landslide risk (about 18.0% of the total), and 34,000 (16.5%) assets have been exposed to medium hazard/probability scenarios [16].

Attention to cultural heritage has always been high. At the international level, several documents have been published about this topic, i.e., the Athens Charter (1934), UNESCO recommendations (1956), and the Venice Charter (1964).

Italian legislation, which until 1970 had followed the international one, moved from it after the seismic events of the 1970s and 1980s. Violent seismic earthquakes revealed the need to develop new methodologies to ensure the safeguarding of heritage resources [17].

From this point, a series of documents have been drawn up in which safeguarding cultural heritage from natural hazards has been associated only to seismic risk, without considering hydrogeological risk assessment. In the last few years, several landslides and avalanches, floods, and other climate-related events have occurred, threatening the conservation of cultural heritage sites. Climate change has already become the most important threat for natural heritage sites, as reported by the latest International Union for Conservation of Nature (IUCN) World Heritage Outlook [18].

The term cultural heritage includes a variety of assets such as natural heritage, monuments, churches, museums, historic villages, and archaeological sites. Among these,

archaeological sites in particular are often located in areas of complex morphology and appear very vulnerable to slope movements.

Originally, the concept of risk for archaeological sites consisted of the evaluation of site relevance, and their protection involved three main purposes: (i) assessing the presence of different assets; (ii) ensuring the integrity of the site in order to increase the number of visitors; (iii) preserving the use of the soil of the site.

Very recently, the normative framework has recognized archaeological assets as a special type of cultural heritage, and the problem of hydrogeological phenomena in archaeological sites was recognized in 2010 with the need to define common approaches to safeguard archaeological heritage from extreme phenomena. The Superior Council Cultural Heritage and Landscape published the first guidelines document for the conservation of archaeological heritage, and for the first time, hydrogeological risk has been considered key for archaeological sites. These guidelines have been applied to the case studies of the archaeological areas of *Ostia Antica* [19] and *Pompeii*. The guidelines for archaeological heritage conservation were aimed at promoting the implementation of all risk mitigation measures for archaeological heritage and improving the fruition of the archaeological sites. Unfortunately, the problem has not been solved and the expectations have not been fulfilled because the conservation of archaeological assets is linked to multiple issues and is not an easy process. For this reason, there are still many archaeological areas for which no methodology able to reduce the vulnerability of the exposed cultural assets has been defined, and there are many sites without defined management and maintenance plans.

In addition, specific aspects such as historical sequences, phases of removal of the material, and soil–structure interaction have to be correlated with geological and geotechnical phenomena [20]. The correlation is an important point to assess the level of risk of the ancient buildings and then to evaluate available strategies to preserve the assets in the future.

Archaeological sites, due to their location, are extremely vulnerable to hydrogeological phenomena and in particular to landslides induced by rainfall. Landslides are able to cause unsettling and ruination of cultural heritage areas; their destructive capacity is generally associated with extraordinary rapidity on a large territory. In spite of this, slow-moving or localized landslides may often gravely damage ancient monuments or archaeological sites [21].

Slopes insisting on monumental assets might be increasingly affected by shallow sliding phenomena as a consequence of climate change. However, the study of the stability conditions of archaeological areas cannot be addressed by conventional procedures, and there are two main aspects to consider: (i) the unavailability of detailed mechanical characterization of soils, as it is conditioned by the presence of interred historical ruins; (ii) the need to plan measures that do not impact the historical context. The first aspect requires the use of a computational method able to incorporate and quantify the uncertainties of the analyzed problem. The second aspect requires adopting mitigation measures in terms of sustainable naturalistic engineering in order to preserve the natural heritage and archaeological sites [22,23].

This paper describes a case study of the archaeological site of Pietrabbondante, a cultural site located in the Molise region (Italy), where slow-moving landslides are compromising the integrity of the ruins. The study focuses on shallow landslide hazard assessment and in particular on the role played by forecasting models of slope stability, for the definition of safeguard strategies. A probabilistic version [24,25] of the transient rainfall infiltration and grid-based slope-stability analysis code (TRIGRS) [26] was used. This version of the code has already been applied in an area located in the Umbria region [27]. The choice to adopt a probabilistic approach with a stochastic evaluation of the stability of the area was due to the impossibility to perform a wide geotechnical investigation campaign in the area (due to the presence of archaeological assets) and to the spatial variability of the mechanical characteristics of the soil. Rainfall-induced landslide hazard scenarios derived from the implementation of a probabilistic forecasting model were analyzed using a series

of projected rainfall events generated by general circulation models (GCMs), following a consolidated approach in landslide-climate studies [28–37].

The paper is organized as follows: In Section 2, a brief historical introduction of the archaeological site is presented together with an overview of the role of geology and geotechnical engineering in the conservation process of the archaeological site, describing the effect of instability phenomena on cultural assets, the characteristics of the soils involved, and details of the geotechnical model. The physically based model and the analyses performed to evaluate the stability of the area are described in Section 3. The results of the simulations are discussed in Section 4, while some concluding remarks are provided in Section 5.

2. The Pietrabbondante Study Area

2.1. Historical and Artistic Framework

The Pietrabbondante area is an important archaeological site located at an altitude of 1000 m a.s.l. in the Isernia province, Molise region (Figure 2a). The site is known for the extraordinary architectural testimonies of Italic Hellenism (Figure 2b). Between the 4th and the 1st century BC, the monument symbolized an important place of a public cult for the Sanniti community. Abandoned during the Hannibalic war, the site was discovered at the end of the Second Punic War (2nd century BC) with the construction of the so-called Temple A (A in Figure 2b) and the Theatre-Temple B (B in Figure 2b).

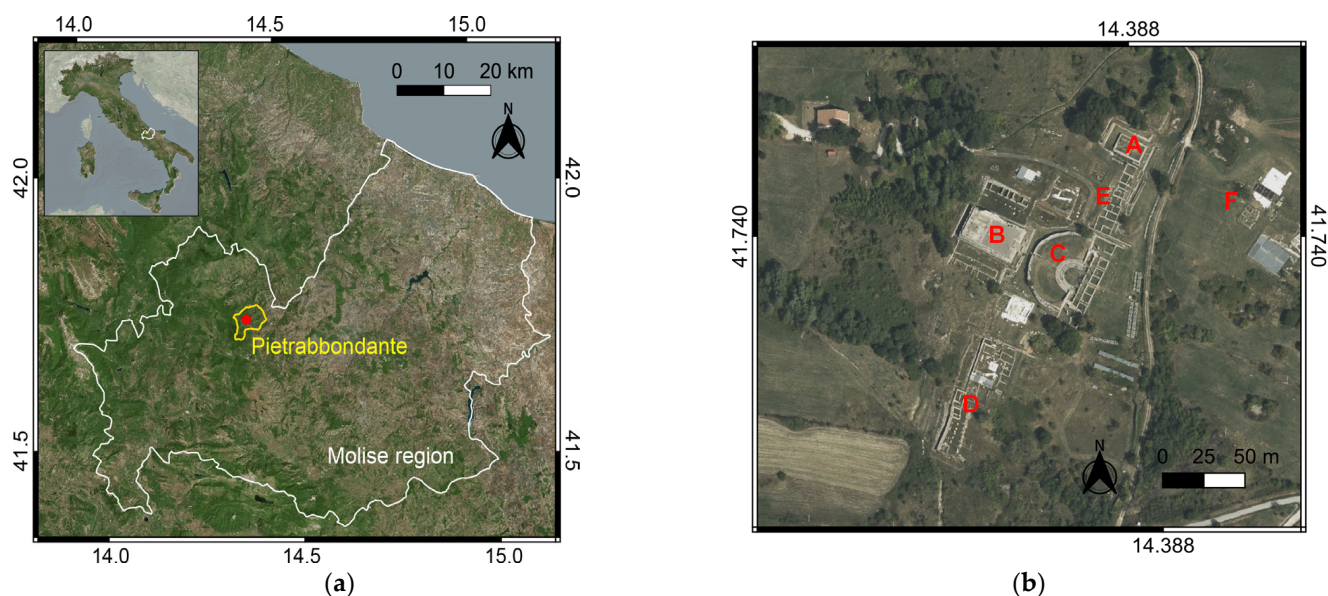


Figure 2. (a) Study area (red point) within the Pietrabbondante municipality (yellow borders) and Molise region (white borders); EPSG:4326. (b) Pietrabbondante area: Minor Temple (A), Major Temple (B), Theatre (C), Public Domus and Stoa (D), Tabernae Area (E), area of new excavations (F). EPSG:4326.

Interest in this majestic archaeological site was born during the Bourbon excavation campaigns (1857–1859), during which Theatre C and Temple A have been discovered.

The Theatre (Figure 3a), the most suggestive place of the monumental area, is located in the center of the archaeological site and has many similarities with the *Teatro Grande of Pompei*. Used to host theatrical performances and political and religious meetings, the monument consists of an upper part (*summa cavea*) and a lower part (*ima cavea*), intended to receive the public. The parts are separated by large blocks of flooring of the time.

It is supposed that the *cavea* had different dimensions, with the presence of wooden seats above the stone ones, still visible today. Temple A (Figure 3b), located on the west side of the archaeological area, was probably erected at the beginning of the 2nd century BC. It

has a single cell structure with a pronaos (a vestibule located at the front of the temple), of which only a podium is preserved.

Located behind the Theatre, on a high podium, is Temple B (Figure 3c). Discovered in 1959, the Temple was probably dedicated to the cult of the Goddess Victory and other sacred figures. It presents a triple cell structure and is composed of a central staircase leading to a paved floor where the altars are accommodated.



(a)



(b)



(c)



(d)

Figure 3. Photos of the main monuments of the archaeological site: (a) Theatre, (b) Temple A, (c) Temple B, (d) Domus Publica.

The number of historical objects recovered in the area demonstrates the religious and political role that the archaeological site played in ancient Sannio. Notable among the several recoveries of recent years are: (i) the *Domus Publica* (Figure 3d), a concrete example of a house at atrium et impluvium, (ii) the *tabernae area*, located on two parallel terraces between Theatre-Temple B complex and Temple A, and (iii) the “unfinished construction site”, an exceptional area north of the Theatre, characterized by the presence of limestone blocks placed in a row and not completed by the stonemasons.

2.2. The Effect of Instability Phenomena on Cultural Assets

The artefacts located in the archaeological site of Pietrabbondante are heterogeneous from typological, constructive, and chronological points of view. Many monuments are incomplete due to restoration and excavation measurements, but others appear deformed by slope movements [28,38] due to the presence of fine-grained soils and erosion mechanisms triggered by run-off phenomena.

In the northwestern sector of the Molise Region where Pietrabbondante is located, the Oligocene-Miocene succession involves the Molise basin formations, namely the Agnone Unit [16,39]. In particular, the archaeological area is situated along the southeastern slope of Monte Saraceno at an altitude of 950–1000 m a.s.l., characterized by a mean slope of about 12%. In this area the “Flysch del Molise”, consisting of synorogenic arenaceous-clayey sediments, crops out the upper member of the Agnone Unit [39,40].

The historic walls located in the northwestern part of the archaeological area have been subjected to evident deformation over time; based on historical reconstructions and studies, the walls surrounding the structures currently appear as shown in Figure 4a, showing the evident effect of the movements on the historical walls in the eastern part of the archaeological area.



Figure 4. The effect of landslides on the archaeological area: (a) damage to the historical walls located in the eastern part of the site; (b) loss of alignment of the columns in the central nave of Domus Colonnade.

Other evident signs of alteration are visible in the *domus colonnade* (Figure 4b). According to historical reconstructions, the colonnade was built with elements of the central nave aligned. Today, the central columns appear to be in advanced positions compared to the rest of the colonnade. In addition, regarding the pillars, phenomena of subsidence of the soil, such as soil creeps and complex movements, are evident [41].

In the new dig area, slope movements contribute to instability of the new discovered structures. Due to these slope movements, it was necessary to install temporary retaining systems, as shown in Figure 5.

Historical analyses reveal that the site has been involved in several landslides in the far and recent past; the archaeological site appeared completely covered by alluvial deposits in the 2nd century AD, and different soil movements caused difficulties during the excavations (Figure 6). Currently, the main gravitational phenomena, both dormant and active, include soil creeps, solifluction, and complex movements (IFFI Project) [41].

Emergency Management in 2006

In the summer of 2006, important archaeological discoveries determined an enlargement of the excavation area including the slope where the *Domus Publica* is located. During the excavations, varied evidence of soil instability was observed, and the Municipality of Pietrabbondante decided to conduct a geotechnical study to define the stability conditions of the archaeological area. The aim of this study was to assess probable risk scenarios and to plan supporting measures to mitigate the risk.

The slope investigated with geotechnical tests is located north of the *Domus Publica* and appeared to be bordered by two runoff gullies. The runoff increased with intense and prolonged weather events and affected the local equilibrium state of shallow soil covers.

Additionally, a slow and shallow viscoplastic deformation has been identified in the area. This deformation appeared to be more active, possibly due to new historical excavations that were conducted without proper planning in recent years.

Studies conducted before 2006 revealed small landslide movements of a few millimeters per year, while in 2006, significant deformations were observed in the areas of *Domus and Sanctuary*, where a temporary retaining system collapsed, due to soil movements. The current movement was recognized as a new landslide area affecting the entire southwestern part of the archaeological area (Figure 7).

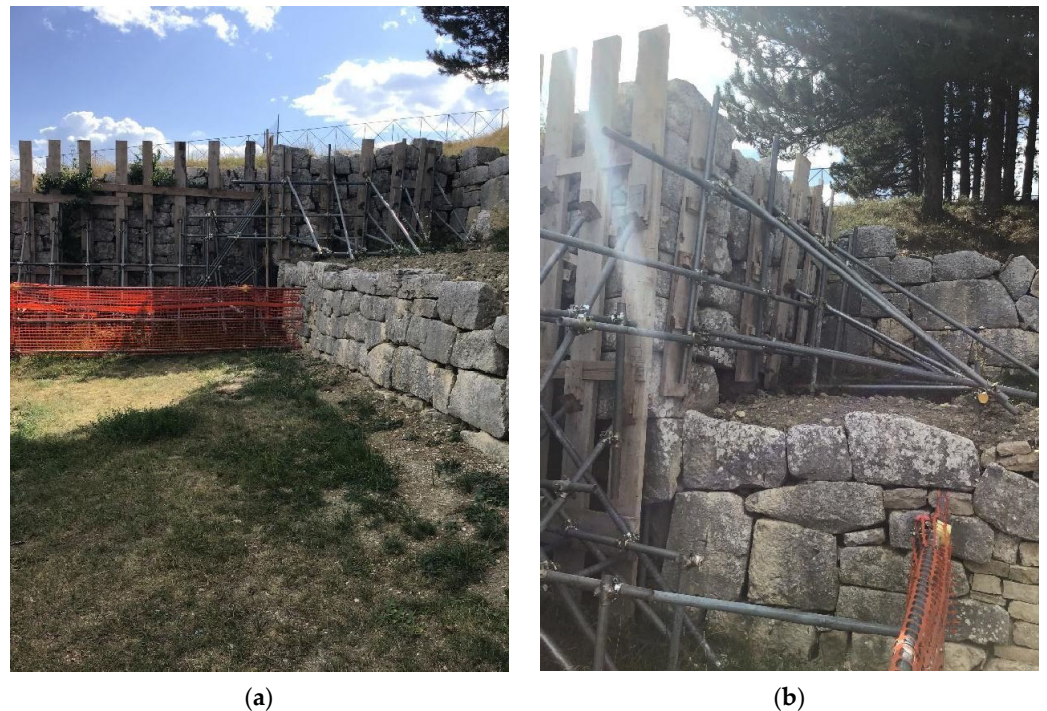


Figure 5. State of the monuments located in the recent area of excavation: temporary retaining systems. (a) overview photo; (b) zoom in detail.



Figure 6. The Theatre as seen in a photo from the archive of National Institute of Archeology and Art History [42].

From the results of the studies carried out in the different periods it can be noticed that the presence of a complex geomorphological scenario is not able to ensure stable conditions for the historical area in the short and long term.

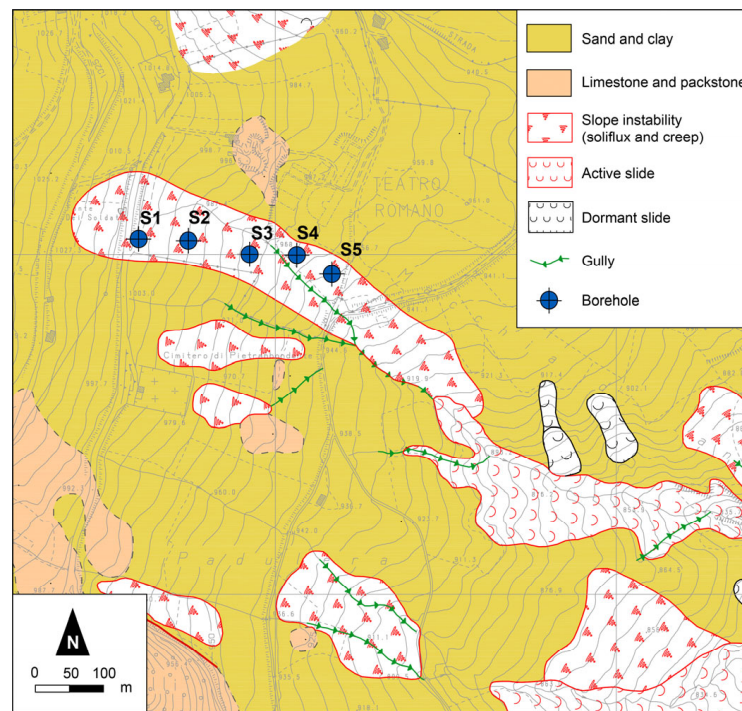


Figure 7. An extract of the geomorpholithological map with a focus on the landslide area affecting the entire southwestern part of the archaeological site, and the position of geotechnical tests: S1–S5 [43].

2.3. Geotechnical Characterization of the Area

The geotechnical investigations performed in 2006 consisted of 12 laboratory soil tests carried out on undisturbed samples derived from 5 boreholes aligned along the direction of maximum slope [44]. Details of the geotechnical laboratory tests and the collected samples’ depth are summarized in Table 1.

Table 1. Program of the geotechnical investigations carried out in 2006.

Borehole	Depth (m)	Laboratory Tests
S1	12.3–12.8	Particle-size analysis Atterberg limits Expansion index test
S2	1.8–2.3	Granulometric analysis Atterberg limits Triaxial shear test (TX-CU) Direct shear test
	5.0–5.5	Granulometric analysis Atterberg limits
S3	1.5–2.0	Granulometric analysis Atterberg limits Lateral expansion test Granulometric analysis Atterberg limits
	4.5–5.0	Triaxial strength test (TX-UU) Direct shear test Lateral expansion test Direct shear test
	5.0–5.5	Granulometric analysis Atterberg limits Lateral expansion test

Table 1. Cont.

Borehole	Depth (m)	Laboratory Tests
S5	1.5–2.0	Granulometric analysis Atterberg limits Triaxial strength test (TX-UU)
	12.0–12.5	Granulometric analysis Atterberg limits Direct shear test
	20.0–20.5	Granulometric analysis Atterberg limits Direct shear test

The results of the geotechnical tests allowed to define the following three homogeneous layers from the ground surface downward:

- Layer A: chaotic colluvial deposits, composed of brown clayey silts embracing plant residues and occasional calcarenitic fragments;
- Layer B: weathered and reworked deposits due to creep and solifluction processes. They consist of brown and grey silty clays characterized by a weak scaly/schistose structure. These deposits embrace organic matter as well as occasional marly and calcarenitic fragments and are often iron-oxidated and decalcified;
- Layer C: grey scaly silty clays interbedded with centimetric to decametric marly and calcarenitic levels.

The profile of the investigated slope is shown in Figure 8. The profile is characterized by the presence of a deformed soil layer that involves a thickness of about 5 m near hole S1. The thickness of soil involved in the landslide is reduced to 2.5 m near hole S5, while in the area upstream of the historic ruins, the mobilized soil reaches thicknesses of 3.2 m.

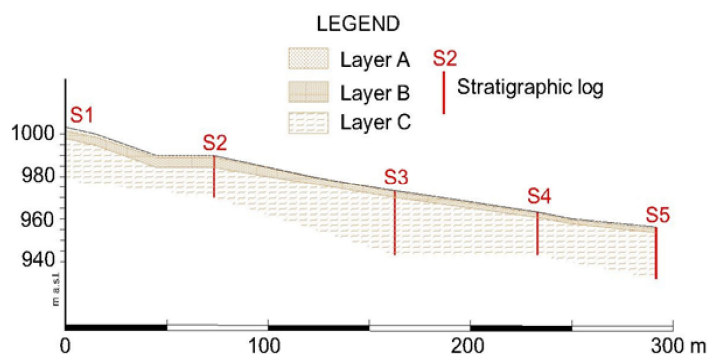


Figure 8. Stratigraphic profile of the analyzed section with the position of geotechnical tests: S1–S5.

3. Description of the Analyses

The methodology applied in this study involved the evaluation of different hazard scenarios that might occur in the archaeological area as a consequence of expected rainfall events. As shown by the results of geotechnical investigations, the landslide threatening the archaeological site involves the most reworked shallow soil thicknesses, influenced by changes in pore water pressure and degree of saturation due to rainfall events.

Future landslide scenarios for the archaeological area were analyzed through a probabilistic approach considering the impossibility of analyzing the progressive failure mechanism based on laboratory and in situ test results due to the presence of underground assets.

The occurrence of a shallow landslide triggered by rainfall was assessed by computing the probability of failure (PoF), defined as the probability of obtaining a factor of safety (FS) lower than 1. The application of the probabilistic approach allows the stochastic determination of the PoF maps, providing a quantitative measure of the stability of the slopes in the area. The PoF maps help understand the portions of the area characterized by medium and high probability of failure, i.e., where landslides are likely to occur.

3.1. Physically Based Landslide Forecasting Model

As already mentioned, the knowledge of the geotechnical soil properties is not enough to define a detailed geotechnical model and use a deterministic analysis approach, which assumes input variables without uncertainties. The modeling of the triggering process of a landslide phenomenon is characterized by different sources of uncertainty, totally ignored by deterministic models, which can never be considered null. Typically, these uncertainties are due to: (i) measurement errors in the geotechnical characterization of the soil; (ii) hypothesis of the mathematical model used to describe the phenomenon; (iii) spatial variability of the mechanical characteristics of the soil. For these reasons, a probabilistic approach was preferred. In particular, the method allows to consider the uncertainty that characterizes the input variables of a stability problem. Soils and rocks are described by parameters characterized by high spatial variability both in horizontal and vertical directions [45]; for instance, mechanical properties show their uncertainty not only from site to site and within a given stratigraphy but also within homogeneous covers as a consequence of natural deposition processes [46]. Probabilistic models allow considering these aspects and modeling the random variables by defining the probability density function (pdf).

The physically based probabilistic model is constructed by coupling a simple hydraulic model for the analysis of the pore pressure evolution during rainfall, and a mechanical model for slope stability evolution due to pore pressure changes [27,47].

The probabilistic model, implemented in order to assess the impact of the pdf definition on the evaluation of the probability of failure (PoF), represents a probabilistic version [27] of the original TRIGRS code [48]. The probabilistic approach is able to work through the discretization of the study area on a regular grid, coupling a hydraulic model for the evolution of pore water pressure in time and a mechanical model for the assessment of the temporal slope stability conditions. In particular, a large-scale analysis was performed, considering the study area discretized into 10 m × 10 m cells.

The hydraulic process is governed by the Richard equation, controlling in 1D conditions the pressure head ψ evolution, while the mechanical model is represented by an infinite slope model [24,26,48]. In transient flow conditions, due to the evolution with time and space of the pressure head ψ generated by the rainfall infiltration process, the classical expression of the factor of safety (FS) used in deterministic analyses varies with depth and time. The evaluation of ψ evolution is based on the solution of the mass conservation equation for solid and liquid phases. Consequently, the stability analysis is controlled by the balance of mass for pore water and requires the definition of several parameters, such as: saturated and residual volumetric water content (θ_s and θ_r), soil stiffness (E_{ed}), initial pre-storm water table depth (d_w), pre-storm infiltration rate parameters (a_α and I_{LT}), thickness of the soil cover (h), and hydraulic conductivity (k_s). Globally, the safety factor F_s depends on the following 12 parameters:

$$F_s = f(\alpha, h, d_w, \gamma_s, c', \varphi', E_{ed}, k_s, \theta_s, \theta_r, a_\alpha, I_{LT}) \quad (1)$$

where α is the slope angle, c' and φ' , respectively, are effective cohesion and friction angle of the soil, and γ_s the unit weight of the soil.

In the stochastic analysis, the stability conditions are expressed by the PoF, depending on the 12 random variables reported in Equation (1). In the present study, the number of random variables was reduced by making appropriate hypotheses, without affecting the forecast reliability. In particular, the following quantities were considered random:

- soil mechanical properties, c' , φ' (hypothesis: γ_s is constant);
- soil saturated hydraulic conductivity k_s and soil stiffness E_{ed} (hypothesis: the soil cover is in fully saturated conditions)
- soil cover layer thickness, h (hypothesis: the high resolution of DTM allows to consider the other geometrical parameters as accurate and without uncertainty).

The reliability analyses were conducted using the Monte Carlo method: based on the pdf distributions, the approach generates pseudo-random numbers for each random quantity. The exact method consists of N deterministic analyses able to define the value assumed by a random dependent variable (PoF in this case) connected to independent random input quantities. N can be expressed as:

$$N = \left(\frac{h_{\alpha/2}}{2\varepsilon} \right)^{2m} \quad (2)$$

where ε is given by the confidence level $1 - \alpha$, and $h_{\alpha/2}$ is the number of standard deviation units between the mean value and that defining the assigned confidence level, and m is the number of variables considered. High confidence levels are required to ensure a good accuracy of the results. More details about the methodology are included in the works [25,27].

3.2. Mechanical Variables

The random variables considered in the mechanical model are: (i) the effective cohesion of soil, (ii) the effective friction angle, (iii) the residual friction angle of soil Φ_r , (iv) saturated hydraulic conductivity, (v) oedometric modulus, and (vi) thickness of soil cover. Random variability was described for each variable by the theoretical probability density function (pdf). The pdf definition was evaluated based on in situ measurements and literature data [49–53].

The mean value of Φ' results from geotechnical tests (Table 1), the mean value of Φ_r derives from the clay fraction (CF) considering Skempton's relation [54], while for the evaluation of the mean value of E_{ed} , literature data were used [55]. The mean value of k_s was obtained from particle size curves available for soil cover through the Kozeny–Carman equations [55–58]. The average thickness of the soil cover (h_i) for each cell of the grid was evaluated using the following expression [41]:

$$h_i = h_{max} - \left(\frac{Z_i - Z_{min}}{Z_{max} - Z} \right) \cdot (h_{max} - h_{min}) \quad (3)$$

where h_{max} and h_{min} refer to the maximum and minimum soil thicknesses, respectively, and Z_{max} and Z_{min} are the maximum and minimum elevations, respectively.

The stochastic characterization of the soil cover of the Pietrabbondante area is summarized in Table 2.

Table 2. Mechanical properties of the soil considered in the slope stability analysis.

Variable	Symbol	Unit	pdf	Mean
Effective friction angle	Φ'	(deg.)	Normal	28
Residual friction angle	Φ_r	(deg.)	Normal	18
Saturated hydraulic conductivity	k_s	(m/s)	Log Normal	1.76×10^{-6}
Oedometric modulus	E_{ed}	(kPa)	Beta	1.00×10^4
Thickness of the soil cover	h	(m)	Gauss distribution	3

In the absence of detailed information or recorded data, the initial pre-storm water table depth (d_w) was set equal to the soil cover thickness, the steady pre-storm infiltration rate (I_{LT}) was assumed to be negligible, and soil thickness did not exceed 4 m. The stability analyses were conducted considering the conservative assumption of the soil cover in saturated conditions ($S_r = 1$).

3.3. Rainfall Data and Variables

Daily rainfall series were gathered from a subset of EURO-CORDEX (Coordinated Downscaling Experiment—European Domain) bias-corrected projections as weather inputs for the assessments included in the PESETA (Projection of Economic impacts of climate

change in Sectors of the European Union based on bottom-up Analysis) initiative [59]. For each dataset, data for the historical period of 1981–2010 as well as for three 30-year periods of 2011–2040, 2041–2070, and 2071–2100 were considered. The series resulted from the dynamical downscaling of five Global Climate Models [60] from the CMIP5 (Coupled Model Intercomparison Project Phase 5), by means of an ensemble of Regional Climate Models (RCMs), at a resolution of 0.11° . The future projections were forced by two Representative Concentration Pathways (RCP), namely RCP 4.5 and RCP 8.5 (the suffix stands for the increase in radiative forcing, in $W \cdot m^{-2}$, at year 2100, with respect to 1765, i.e., the pre-industrial period). RCMs' outputs were bias-adjusted using the methodology described in [61] and the observational data set EOBSv10 [62,63].

The following datasets were used in this work:

1. CNRM-CERFACS-CNRM-CM5_r1i1p1_CLMcom-CCLM4-8-17, hereinafter H1;
2. ICHEC-EC-EARTH_r12i1p1_CLMcom-CCLM4-8-17, hereinafter H2;
3. IPSL-IPSL-CM5A-MR_r1i1p1_IPSL-INERIS-WRF331F, hereinafter H3;
4. MOHC-HadGEM2-ES_r1i1p1_SMHI-RCA4, hereinafter H4;
5. MPI-M-MPI-ESM-LR_r1i1p1_SMHI-RCA4, hereinafter H5.

Figures 9 and 10 show the values of average seasonal rainfall and maximum daily rainfall in the historical period of 1981–2010 as well as for the three periods of 2011–2040, 2041–2070, and 2071–2100, for the five models and the two concentration scenarios considered in this study. Values were grouped by the seasons used in climatological analysis, i.e., DJF (December–January–February), MAM (March–April–May), JJA (June–July–August), SON (September–October–November). Overall, in the studied area, less rainfall is expected in JJA and more rainfall is expected in SON (particularly according to RCP 4.5) and in MAM (especially according to H4 model). On the other hand, maximum daily rainfall is expected to increase in the RCP 8.5 scenario, particularly in JJA and SON seasons.

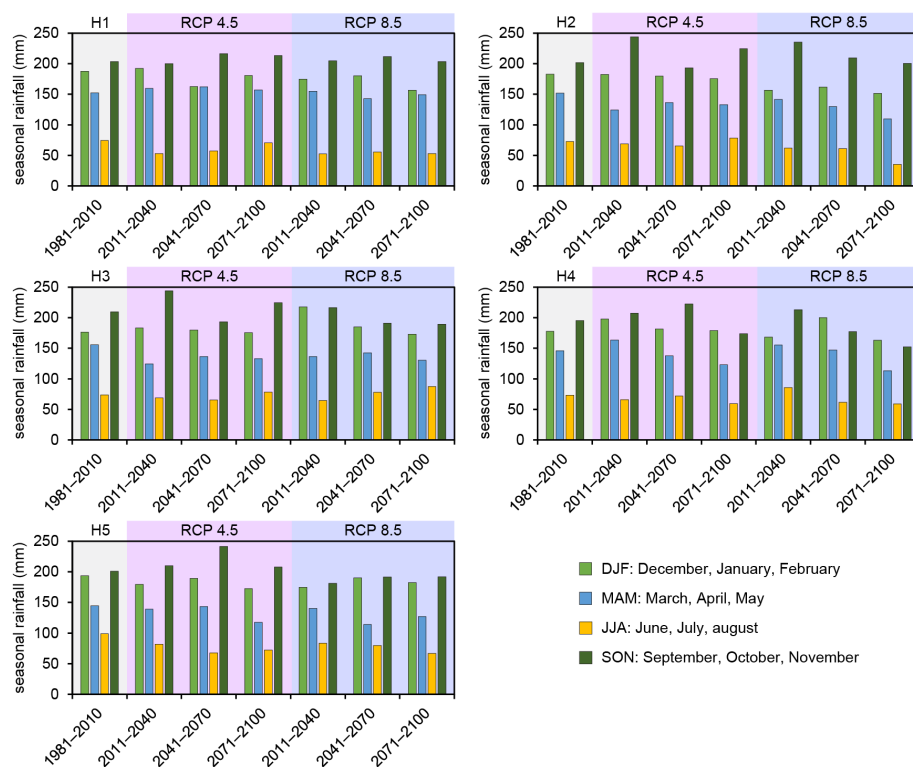


Figure 9. Mean seasonal rainfall values in the study area for the historical period of 1981–2010 and the future periods of 2011–2040, 2041–2070, and 2071–2100, according to the five models (H1–H5) and the two concentration scenarios (RCP 4.5—bars on pink backcolor, RCP 8.5—bars on violet backcolor) considered in this study.

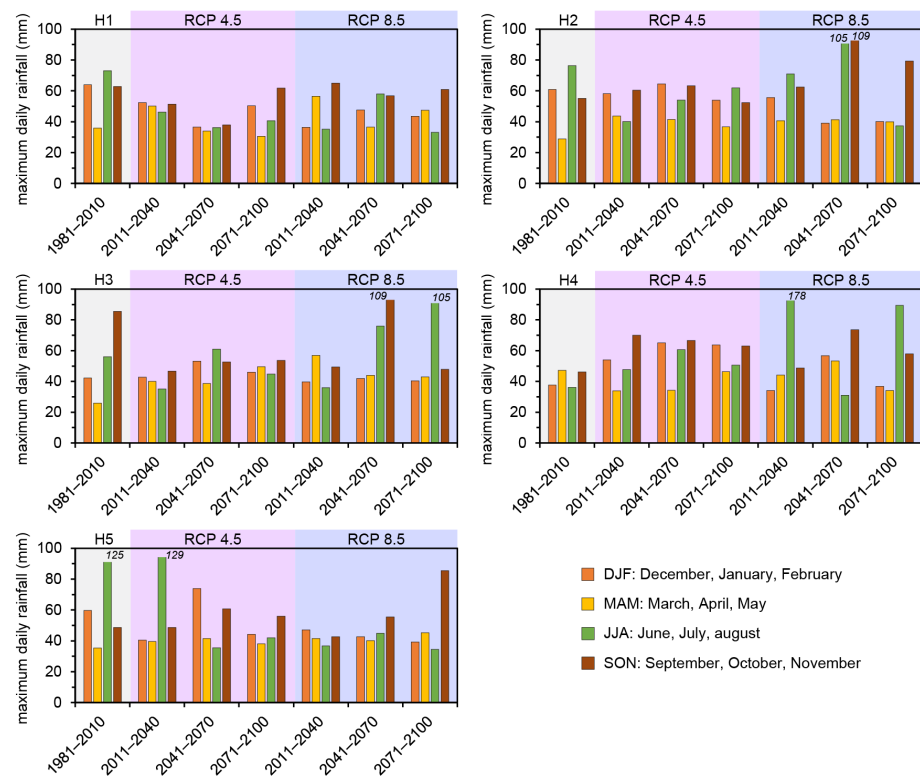


Figure 10. Maximum daily rainfall values in the study area for the historical period of 1981–2010 and the future periods of 2011–2040, 2041–2070, and 2071–2100, according to the five models (H1–H5) and the two concentration scenarios (RCP 4.5—bars on pink backcolor, RCP 8.5—bars on violet backcolor) considered in this study. The values were grouped into four seasons.

Table 3 summarizes the main features of the considered datasets in terms of average values and coefficients of variation of rainfall intensity.

Table 3. Main features of the 5 considered rainfall datasets. For each temporal horizon and RCP, the average value (AV), in mm/day, and the coefficient of variation (COV) are reported.

Dataset ID	2011–2040		RCP 4.5 2041–2070		2071–2100		2011–2040		RCP 8.5 2041–2070		2071–2100	
	AV	COV	AV	COV	AV	COV	AV	COV	AV	COV	AV	COV
H1	1.7	2.52	1.6	2.42	1.7	2.49	1.6	2.50	1.6	2.51	1.5	2.69
H2	1.7	2.59	1.6	2.63	1.7	2.69	1.6	2.66	1.5	2.84	1.4	3.03
H3	1.7	2.44	1.8	2.47	1.7	2.47	1.7	2.44	1.6	2.67	1.6	2.62
H4	1.7	2.46	1.7	2.56	1.6	2.69	1.7	2.66	1.6	2.65	1.4	2.83
H5	1.7	2.45	1.8	2.41	1.6	2.53	1.6	2.44	1.6	2.49	1.6	2.62

Rainfall is available for future periods with a daily temporal resolution. Therefore, events of 24 h in duration and constant average intensity were considered. Rainfall intensity is considered a random variable for the model described by a lognormal pdf. The average intensities were similar for both models (Table 3), as were the coefficients of variation (COV). This was due to averaging the rainfall data at the daily timestep. However, given the high value of the cultural assets, this precautionary assumption could be considered as acceptable. Some results obtained in relation to the period of 2041–2070 and the H5 model only by considering the average intensity values provided by the RCP 4.5 and RCP 8.5 are shown. In addition, stability analyses were performed considering the maximum intensities observed for RCP 4.5 corresponding to H5 ($i_{\max 4.5} = 73.9 \text{ mm} - 3 \text{ mm/h}$) and for the RCP 8.5 model corresponding to H5 ($i_{\max 8.5} = 55 \text{ mm} - 2.29 \text{ mm/h}$).

4. Results

To observe the effect of the rainfall on the model of spatially distributed predictions, the PoF spatial distributions obtained for the archaeological site considering the average rainfall intensities is shown in Figure 11a,b. The figures show that the spatial distribution of the PoF at the archaeological site and around the study area was approximately the same. Considering average rainfall intensities of $i_{4,5}$ and $i_{8,5}$, PoFs < 25% were obtained over an extended area in the north of the *Domus* and also in the area already subjected to a landslide (Inside the polygon).

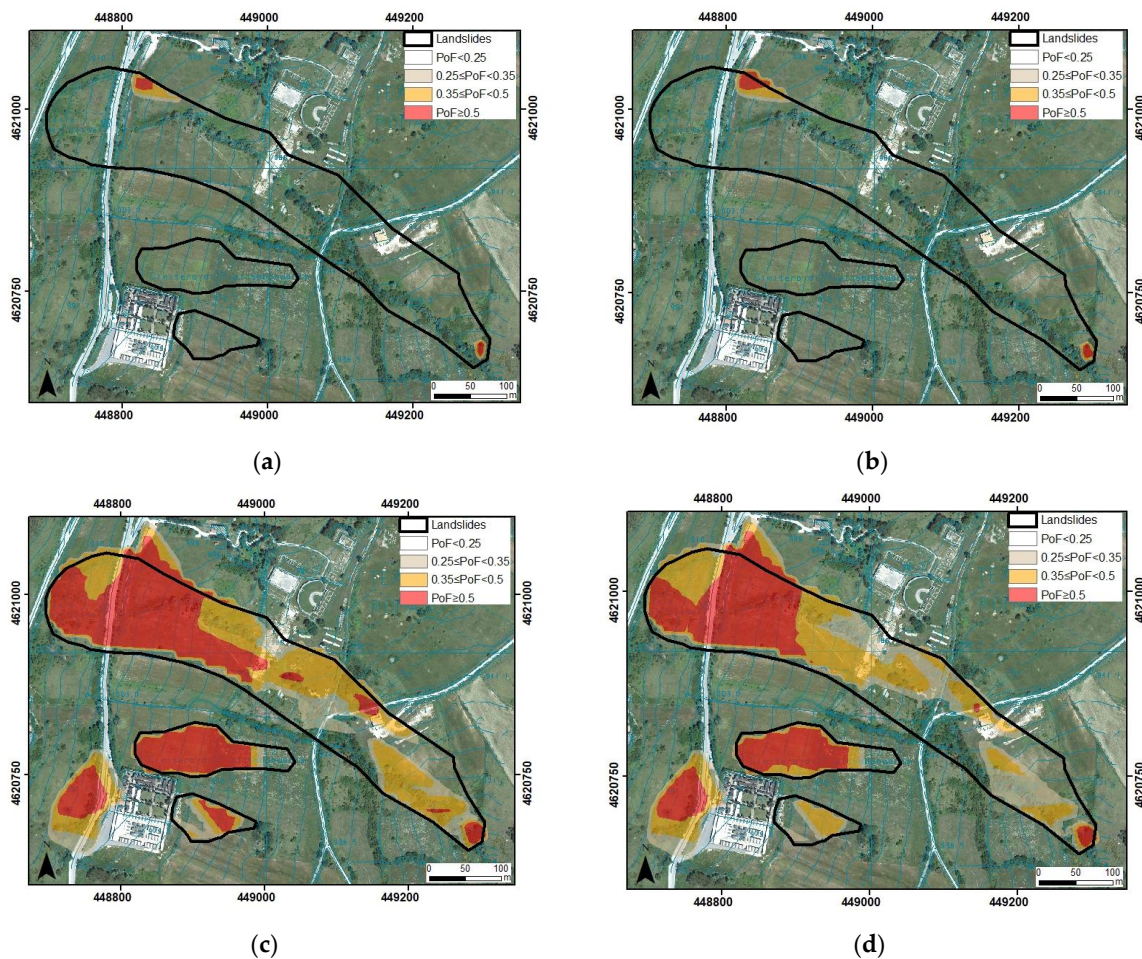


Figure 11. Spatial distributions of the PoF in relation to rainfall intensities in the 2041–2040 period: (a) rainfall $i_{4,5}$; (b) rainfall $i_{8,5}$; (c) rainfall $i_{max4.5}$; (d) rainfall $i_{max8.5}$.

Figure 11a,b shows the presence of a small area in the northwest located north of Theater-Temple B and a small area in the southeast characterized by values of the PoF $\geq 35\%$ (red and orange areas). As expected, these values of the PoF characterize more sloping areas within the polygon of the occurred landslides.

Clearer differences in terms of the PoF could be noticed by analyzing the results of the analyses carried out by adopting the maximum rainfall intensities as input data. Figure 11c,d shows the PoF values obtained in the analyses considering the maximum rainfall intensity $i_{max4.5} = 3 \text{ mm/h}$ from the dataset RCP 4.5 (Figure 11c) and the maximum rainfall intensity $i_{max8.5} = 2.29 \text{ mm/h}$ from the dataset RCP 8.5 (Figure 11d), both related to the H5 model and the 2041–2070 period.

Figure 11c,d shows large areas characterized by medium-high values of the PoF. The spatial distribution of the medium-high values of the PoF reproduces the form of the polygon delimiting the areas where landslides occurred. Moreover, both figures show a further area (in the southwest) where landslides have not been registered in the past

that would become unstable if the maximum rain intensity reached the values assumed in these analyses.

In detail, Figure 11c shows a larger area characterized by medium-high probability of failure ($35\% \leq \text{PoF} \leq 50\%$) within the landslide polygon (orange area). The red area characterized by a high probability of failure ($\text{PoF} \geq 50\%$) was also revealed to be very extensive. In Figure 11d, portions of red areas of Figure 11c correspond to orange areas, characterized by medium-high probability of failure. The most external landslide polygon from Figure 11c,d had medium-high probability of failure values $\geq 35\%$.

In any case, the probability of failure appeared to be significant in the archaeological area and not negligible even in areas not identified as affected by shallow movements in the past.

The effect of rainfall events on the stability conditions of the area was highlighted by comparing the results reported in Figure 11. In fact, areas characterized by a medium-high probability of failure obtained when considering maximum rainfall intensities (Figure 11c,d) had low values of the PoF when average rainfall intensities were considered (Figure 11a,b). In particular, in the case of the more dangerous classes (red classes), it can be noticed that red PoF cells were about 9% (Figure 11c) and 7% (Figure 11d) of the total cells of the area, while red PoF cells were significantly smaller (about 0.2% in Figure 11a and 0.3% in Figure 11b). Similar evidence could be observed by comparing the cells characterized by medium PoF values (orange): Figure 11a,b, respectively, show 0.1% and 0.2% of orange cells, while in Figure 11c,d the percentages of the orange cells are about 6% of the total cells of the area.

5. Conclusions

This paper focuses on rainfall-induced landslide hazard assessment of an archaeological heritage located in the site of Pietrabbondante (Italy) from a climate change perspective. The impact of the expected rainfall regimes on slope stability conditions was evaluated through the application of a probabilistic, physically based approach in which the physical process that leads to slope failure was characterized by multiple uncertainties and the safety level of the slope was expressed as a random variable, quantified by the probability of failure (PoF). Reliability analyses were conducted using the Monte Carlo method to generate pseudo-random numbers for each random quantity based on the pdf distributions.

The rainfall events considered as inputs in the probabilistic physically based landslide model were characterized by average/maximum intensity values provided by two Representative Concentration Pathways (RCP), namely RCP 4.5 and RCP 8.5, derived from the daily rainfall series gathered from a subset of EURO-CORDEX projections.

The results showed that large portions of the Pietrabbondante area were characterized by a medium-high probability of failure, especially when subjected to the maximum intensities of the considered rainfall data, that was not negligible even in the case of the small average daily intensities. These results are key because extreme rainfall events may become more frequent and intense in the area according to the expected climate projections. Extreme rainfall events characterized by high maximum intensity (also with short duration), as recently occurred in Italy and in many European countries, and their suddenness, can consequently lead to an increase in shallow landslides in an important archaeological heritage site in the central Italy.

In order to study this aspect, fully coupled two-dimensional FEM analyses will be carried out in future research considering extreme rainfall events as an input and evaluating their effect on the stability conditions of the single slopes of the Pietrabbondante area.

Author Contributions: Conceptualization, E.V., S.L.G. and E.C.; methodology, E.V. and Y.P.; writing—original draft preparation, E.V. and Y.P.; writing—review and editing, E.C. and S.L.G.; supervision, E.C., S.L.G. and L.C. All authors have read and agreed to the published version of the manuscript.

Funding: This research received no external funding

Data Availability Statement: The data presented in this study are available on request from the corresponding author.

Acknowledgments: The authors thank Guido Rianna and Alfredo Reder (CMCC, Italy) for their support in gathering the EURO-CORDEX data.

Conflicts of Interest: The authors declare no conflict of interest.

References

- Shirvani Dastgerdi, A.; Sargolini, M.; Broussard Allred, S.; Chatrchyan, A.; De Luca, G. Climate change and sustaining heritage resources: A framework for boosting cultural and natural heritage conservation in Central Italy. *Climate* **2020**, *8*, 26. [[CrossRef](#)]
- Salciarini, D.; Brocca, L.; Camici, L.; Ciabatta, L.; Volpe, E.; Massini, R.; Tamagnini, C. Physically based approach for rainfall-induced landslide projections in a changing climate. *Proc. Inst. Civ. Eng. Geotech. Eng.* **2019**, *172*, 481–490. [[CrossRef](#)]
- Salciarini, D.; Volpe, E.; Kelley, S.; Brocca, L.; Camici, S.; Fanelli, G.; Tamagnini, C. Modeling the Effects Induced by the Expected Climatic Trends on Landslide Activity at Large Scale. In Proceedings of the 6th Italian Conference of Researchers in Geotechnical Engineering, CNRIG 2016, Bologna, Italy, 22–23 September 2016; Volume 158, pp. 541–545, Code 123733.
- Sabbioni, C.; Cassar, M.; Brimblecombe, P.; Tidblad, J.; Kozłowski, R.; Drdácý, M.; Saiz-Jimenez, C.; Grøntoft, T.; Wainwright, I.; Ariño, X. Global climate change impact on built heritage and cultural landscapes. In Proceedings of the International Conference on Heritage, Weathering and Conservation, HWC 2006, Madrid, Spain, 21–24 June 2006; pp. 395–401.
- Fatorić, S.; Seekamp, E. Are cultural heritage and resources threatened by climate change? A systematic literature review. *Clim. Chang.* **2017**, *142*, 227–254. [[CrossRef](#)]
- Guzzetti, F.; Gariano, S.L.; Peruccacci, S.; Brunetti, M.T.; Melillo, M. Rainfall and landslide initiation. In *Rainfall*; Elsevier: Amsterdam, The Netherlands, 2022; pp. 427–450.
- Comegna, L.; Damiano, E.; Greco, R.; Guida, A.; Olivares, L.; Picarelli, L. Field hydrological monitoring of a sloping shallow pyroclastic deposit. *Can. Geotech. J.* **2016**, *53*, 1125–1137. [[CrossRef](#)]
- Cigna, F.; Harrison, A.; Tapete, D.; Lee, K. Understanding geohazards in the UNESCO WHL site of the Derwent Valley Mills (UK) using geological and remote sensing data. In Proceedings of the Fourth International Conference on Remote Sensing and Geoinformation of the Environment (RSCy2016), Paphos, Cyprus, 4–8 April 2016; SPIE: Bellingham, WA, USA, 2016; pp. 604–613.
- Margottini, C.; Gigli, G.; Ruther, H.; Spizzichino, D. Advances in geotechnical investigations and monitoring in rupestrian settlements inscribed in the UNESCO's World Heritage List. *Procedia Earth Planet. Sci.* **2016**, *16*, 35–51. [[CrossRef](#)]
- Ravankhah, M.; de Wit, R.; Argyriou, A.V.; Chliaoutakis, A.; Revez, M.J.; Birkmann, J.; Žuvela-Aloise, M.; Sarris, A.; Tzigounaki, A.; Giapitsoglou, K. Integrated assessment of natural hazards, including climate change's influences, for cultural heritage sites: The case of the historic centre of Rethymno in Greece. *Int. J. Disaster Risk Sci.* **2019**, *10*, 343–361. [[CrossRef](#)]
- Zollo, A.L.; Rianna, G.; Mercogliano, P.; Tommasi, P.; Comegna, L. Validation of a Simulation Chain to Assess Climate Change Impact on Precipitation Induced Landslides. In *Landslide Science for a Safer Geoenvironment*; Sassa, K., Canuti, P., Yin, Y., Eds.; Springer International Publishing: Cham, Switzerland, 2014; pp. 287–292.
- Sabbioni, C.; Brimblecombe, P.; Cassar, M. *The Atlas of Climate Change Impact on European Cultural Heritage: Scientific Analysis and Management Strategies*; Anthem Press: London, UK, 2010.
- Rianna, G.; Zollo, A.; Tommasi, P.; Paciucci, M.; Comegna, L.; Mercogliano, P. Evaluation of the effects of climate changes on landslide activity of Orvieto clayey slope. *Procedia Earth Planet. Sci.* **2014**, *9*, 54–63. [[CrossRef](#)]
- Sesana, E.; Gagnon, A.S.; Ciantelli, C.; Cassar, J.; Hughes, J.J. Climate change impacts on cultural heritage: A literature review. *Wiley Interdiscip. Rev. Clim. Chang.* **2021**, *12*, e710. [[CrossRef](#)]
- Trigila, A.; Frattini, P.; Casagli, N.; Catani, F.; Crosta, G.; Esposito, C.; Iadanza, C.; Lagomarsino, D.; Mugnozza, G.S.; Segoni, S.; et al. Landslide susceptibility mapping at national scale: The Italian case study. In *Landslide Science and Practice: Volume 1: Landslide Inventory and Susceptibility and Hazard Zoning*; Springer: Berlin/Heidelberg, Germany, 2013; pp. 287–295.
- Braca, G.; Bussetini, M.; Lastoria, B.; Mariani, S.; Piva, F. *Il Bilancio Idrologico Gis Based a Scala Nazionale Su Griglia Regolare-BIGBANG: Metodologia e Stime. Rapporto Sulla Disponibilità Naturale Della Risorsa Idrica*; ISPRA: Rome, Italy, 2021. (In Italian)
- Walters, R.J.; Elliott, J.R.; D'Agostino, N.; England, P.C.; Hunstad, I.; Jackson, J.A.; Parsons, B.; Phillips, R.J.; Roberts, G. The 2009 L'Aquila earthquake (central Italy): A source mechanism and implications for seismic hazard. *Geophys. Res. Lett.* **2009**, *36*. [[CrossRef](#)]
- Osipova, E.; Emslie-Smith, M.; Osti, M.; Murai, M.; Åberg, U.; Shadie, P. *IUCN World Heritage Outlook 3*; IUCN: Gland, Switzerland, 2020; ISBN 978-2-8317-2085-2.
- Cecchi, R.; Gasparoli, P. Attività di prevenzione e cura su un patrimonio di eccellenza: Il caso delle aree archeologiche di Roma e Ostia Antica. *Pensare La Prev.* **2010**, 1–10.
- Lollino, G.; Arattano, M.; Allasia, P.; Giordan, D. Time response of a landslide to meteorological events. *Nat. Hazards Earth Syst. Sci.* **2006**, *6*, 179–184. [[CrossRef](#)]
- Canuti, P.; Margottini, C.; Fanti, R.; Bromhead, E.N. Cultural heritage and landslides: Research for risk prevention and conservation. In *Landslides—Disaster Risk Reduction*; Sassa, K., Canuti, P., Eds.; Springer: Berlin/Heidelberg, Germany, 2009; pp. 401–433.

22. Salciarini, D.; Volpe, E.; Di Pietro, L.; Cattoni, E. A case-study of sustainable countermeasures against shallow landslides in central Italy. *Geosciences* **2020**, *10*, 130. [CrossRef]
23. Cecconi, M.; Pane, V.; Napoli, P.; Cattoni, E. Deep roots planting for surface slope protection. *Electron. J. Geotech. Eng. U* **2012**, *17*, 2809–2820.
24. Salciarini, D.; Fanelli, G.; Tamagnini, C. A probabilistic model for rainfall—Induced shallow landslide prediction at the regional scale. *Landslides* **2017**, *14*, 1731–1746. [CrossRef]
25. Salciarini, D.; Volpe, E.; Cattoni, E. Probabilistic vs. deterministic approach in landslide triggering prediction at large-scale. In *Geotechnical Research for Land Protection and Development: Proceedings of CNRIG, Lecco, Italy, 3–5 July 2019*; Springer: Berlin/Heidelberg, Germany, 2020; pp. 62–70.
26. Baum, R.L.; Savage, W.Z.; Godt, J.W. *TRIGRS: A Fortran Program for Transient Rainfall Infiltration and Grid-Based Regional Slope Stability Analysis, Version 2.0*; US Geological Survey: Reston, VA, USA, 2008.
27. Volpe, E.; Ciabatta, L.; Salciarini, D.; Camici, S.; Cattoni, E.; Brocca, L. The impact of probability density functions assessment on model performance for slope stability analysis. *Geosciences* **2021**, *11*, 322. [CrossRef]
28. Gariano, S.L.; Guzzetti, F. Landslides in a changing climate. *Earth Sci Rev.* **2016**, *162*, 227–252. [CrossRef]
29. Gariano, S.L.; Guzzetti, F. Mass-movements and climate change. *Treatise Geomorphol. Second. Ed.* **2022**, *5*, 546–558. [CrossRef]
30. Ciabatta, L.; Camici, S.; Brocca, L.; Ponziani, F.; Stelluti, M.; Berni, N.; Moramarco, T. Assessing the impact of climate-change scenarios on landslide occurrence in Umbria Region, Italy. *J. Hydrol.* **2016**, *541*, 285–295. [CrossRef]
31. Peres, D.J.; Cancelliere, A. Modeling impacts of climate change on return period of landslide triggering. *J. Hydrol.* **2018**, *567*, 420–434. [CrossRef]
32. He, S.; Wang, J.; Wang, H. Projection of Landslides in China during the 21st Century under the RCP8.5 Scenario. *J. Meteorol. Res.* **2019**, *33*, 138–148. [CrossRef]
33. Lin, Q.; Wang, Y.; Glade, T.; Zhang, J.; Zhang, Y. Assessing the spatiotemporal impact of climate change on event rainfall characteristics influencing landslide occurrences based on multiple GCM projections in China. *Clim. Chang.* **2020**, *162*, 761–779. [CrossRef]
34. Lin, Q.; Steger, S.; Pittore, M.; Zhang, J.; Wang, L.; Jiang, T.; Wang, Y. Evaluation of potential changes in landslide susceptibility and landslide occurrence frequency in China under climate change. *Sci. Total Environ.* **2022**, *850*, 158049. [CrossRef]
35. Araújo, J.R.; Ramos, A.M.; Soares, P.M.M.; Melo, R.; Oliveira, S.C.; Trigo, R.M. Impact of extreme rainfall events on landslide activity in Portugal under climate change scenarios. *Landslides* **2022**, *19*, 2279–2293. [CrossRef]
36. Jakob, M. Landslides in a changing climate. In *Landslide Hazards, Risks, and Disasters*; Elsevier: Amsterdam, The Netherlands, 2022; pp. 505–579.
37. Alvioli, M.; Melillo, M.; Guzzetti, F.; Rossi, M.; Palazzi, E.; von Hardenberg, J.; Brunetti, M.T.; Peruccacci, S. Implications of climate change on landslide hazard in Central Italy. *Sci. Total Environ.* **2018**, *630*, 1528–1543. [CrossRef]
38. Volpe, E.; Marra, A.; La Regina, A.; Fabbrocino, G. A multidisciplinary approach to the safety assessment of the archaeological site of Pietrabbondante. In *Proceedings of the IMEKO International Conference on Metrology for Archaeology and Cultural Heritage, MetroArchaeo, Lecce, Italy, 23–25 October 2017*; International Measurement Confederation (IMEKO): Budapest, Hungary, 2019; pp. 274–279.
39. Patacca, E.; Scandone, P. Geology of the southern Apennines. *Boll. Della Soc. Geol. Ital.* **2007**, *7*, 75–119.
40. Robustelli, G.; Corbi, I.; De Silvio, D. *Carta Geologica d'Italia in Scala 1:50.000-Foglio 393 Trivento*; Ispra: Rome, Italy, 2010.
41. Trigila, A.; Iadanza, C.; Guerrieri, L. The IFFI project (Italian landslide inventory): Methodology and results. *Guidel. Mapp. Areas Risk Landslides Eur.* **2007**, *23*, 15.
42. National Institute of Archeology and Art History. 2023. Available online: <https://www.inasaroma.org/patrimonio/archivio-storico> (accessed on 17 September 2014).
43. Comune di Pietrabbondante. *Piano di Riqualificazione Territoriale in Variante al Vigente Piano di Fabbricazione*; Comune di Pietrabbondante: Pietrabbondante, Italy, 2019.
44. Studio Tecnico Associato di Geologia Applicata Geoconsul. *Progettazione del Complesso Archeologico di Pietrabbondante*; Studio Tecnico Associato di Geologia Applicata Geoconsul: Pietrabbondante, Italy, 2007.
45. Fenton, G.A.; Griffiths, D.V. *Risk Assessment in Geotechnical Engineering*; John Wiley & Sons: New York, NY, USA, 2008; Volume 461.
46. Lacasse, S.; Nadim, F. Model uncertainty in pile axial capacity calculations. In *Offshore Technology Conference*; OnePetro: Richardson, TX, USA, 1996.
47. Raia, S.; Alvioli, M.; Rossi, M.; Baum, R.L.; Godt, J.W.; Guzzetti, F. Improving predictive power of physically based rainfall-induced shallow landslide models: A probabilistic approach. *Geosci. Model. Dev.* **2014**, *7*, 495–514. [CrossRef]
48. Baum, R.L.; Savage, W.Z.; Godt, J.W. *TRIGRS—A Fortran Program for Transient Rainfall Infiltration and Grid-Based Regional Slope Stability Analysis*; US Geological Survey open-file report 424; US Geological Survey: Reston, VA, USA, 2002; Volume 38.
49. De Ghislain, M. *Quantitative Hydrogeology; Groundwater Hydrology for Engineers*; U.S. Department of Energy Office of Scientific and Technical Information: Oak Ridge, TN, USA, 1986.
50. Tobutt, D.C. Monte Carlo simulation methods for slope stability. *Comput. Geosci.* **1982**, *8*, 199–208. [CrossRef]
51. Baecher, G.B.; Christian, J.T. *Reliability and Statistics in Geotechnical Engineering*; John Wiley & Sons: Hoboken, NJ, USA, 2005.
52. Lumb, P. Safety factors and the probability distribution of soil strength. *Can. Geotech. J.* **1970**, *7*, 225–242. [CrossRef]
53. Skempton, A.W. Residual strength of clays in landslides, folded strata and the laboratory. *Geotechnique* **1985**, *35*, 3–18. [CrossRef]

54. Bowles, J.E. *Foundation Analysis and Design*; McGraw-Hill: New York, NY, USA, 1996.
55. Carman, P.C. Fluid flow through granular beds. *Trans. Inst. Chem. Eng.* **1937**, *75*, 150–166.
56. Carman, P.C. Determination of the specific surface of powders. *J. Soc. Chem. Ind. Trans.* **1938**, *CVII*, 225.
57. Carman, P.C. Permeability of saturated sands, soils and clays. *J. Agric. Sci.* **1939**, *29*, 263–273. [[CrossRef](#)]
58. Carman, P.C. *Flow of Gases through Porous Media*; Butterworths: London, UK, 1956.
59. Dosio, A. *EU High Resolution Temperature and Precipitation*; European Commission, Joint Research Centre (JRC): Brussels, Belgium, 2018. Available online: <http://data.europa.eu/89h/jrc-liscoast-10011> (accessed on 17 September 2014).
60. Dosio, A. Projections of climate change indices of temperature and precipitation from an ensemble of bias-adjusted high-resolution EURO-CORDEX regional climate models. *J. Geophys. Res. Atmos.* **2016**, *121*, 5488–5511. [[CrossRef](#)]
61. Dosio, A.; Paruolo, P.; Rojas, R. Bias correction of the ENSEMBLES high resolution climate change projections for use by impact models: Analysis of the climate change signal. *J. Geophys. Res. Atmos.* **2012**, *117*. [[CrossRef](#)]
62. Dosio, A.; Fischer, E.M. Will half a degree make a difference? Robust projections of indices of mean and extreme climate in Europe under 1.5 C, 2 C, and 3 C global warming. *Geophys. Res. Lett.* **2018**, *45*, 935–944. [[CrossRef](#)]
63. Haylock, M.R.; Hofstra, N.; Klein Tank, A.M.G.; Klok, E.J.; Jones, P.D.; New, M. A European daily high-resolution gridded data set of surface temperature and precipitation for 1950–2006. *J. Geophys. Res. Atmos.* **2008**, *113*, D20119. [[CrossRef](#)]

Disclaimer/Publisher’s Note: The statements, opinions and data contained in all publications are solely those of the individual author(s) and contributor(s) and not of MDPI and/or the editor(s). MDPI and/or the editor(s) disclaim responsibility for any injury to people or property resulting from any ideas, methods, instructions or products referred to in the content.